

Correlations of Electrons from Heavy Flavor Decay with Hadrons at PHENIX

Anne Sickles¹ for the PHENIX Collaboration

¹ Brookhaven National Laboratory,
Upton, NY 11973

Abstract. One unexpected recent result from heavy-ion collisions is the large suppression and elliptic flow of electrons from heavy flavor decay. Further measurements of properties of electrons from heavy flavor decay are crucial to understanding the origin of this suppression and its implications for the properties of the hot matter produced at RHIC. Two particle correlations have been used extensively to study the propagation of hard partons through the produced matter in heavy-ion collisions. Measurements in p+p collisions are important both as reference for heavy ion measurements and to study heavy flavor production and fragmentation in the vacuum. Preliminary results of correlations between electrons from heavy flavor decay with charged hadrons from p+p collisions are shown.

Keywords: list of keywords, relevant to the article

PACS: specifications see, e.g. <http://www.aip.org/pacs/>

1. Introduction

Two particle azimuthal correlations at the Relativistic Heavy Ion Collider have been shown to be enormously powerful to study the propagation of jet partons through the hot nuclear matter produced in nucleus-nucleus collisions. The same measurements in proton-proton collisions provide an essential baseline for interpreting heavy ion results and have also been interesting in understanding jet fragmentation [1].

As of now these jet-induced correlations have only involved light hadrons. However, with recent results showing the suppression of electrons from the decay of charm and bottom mesons at a level similar to that of π^0 [2] there is great interest in looking at the correlations of these electrons with other hadrons in the event to study their jet structure and how it differs from that observed in proton-proton collisions and also from the jet structure of light hadron jet correlations. The proton-proton collisions are especially necessary for heavy flavor correlations because the

measured electron is a decay product, thus hadrons from the heavy meson decay contribute to the correlations in addition to other fragmentation products.

2. Analysis Method

Studies of electrons from heavy flavor decay are complicated by the large background of electrons from light meson decay and photon conversions. In this analysis we statistically subtract the correlations from these photonic sources using a method similar to that used to measure direct photon-hadron correlations [3]. What is measured is the inclusive electron-hadron conditional hadron yields per trigger electron, $Y_{e_{incl}-h}$. This is a weighted average of conditional yields hadrons associated with electrons from electrons from heavy flavor decay and the conditional yield of hadrons associated with electrons from photonic sources:

$$Y_{e_{incl}-h} = \frac{N_{e_{HF}} Y_{e_{HF}-h} + N_{e_{phot}} Y_{e_{phot}-h}}{N_{e_{HF}} + N_{e_{phot}}} \quad (1)$$

$Y_{e_{HF}-h}$ is then given by:

$$Y_{e_{HF}-h} = \frac{(R_{HF} + 1)Y_{e_{incl}-h} - Y_{e_{phot}-h}}{R_{HF}} \quad (2)$$

where $R_{HF} \equiv \frac{N_{e_{HF}}}{N_{e_{phot}}}$ and is taken from the published PHENIX measurement [4] for the electron p_T bins used in this analysis.

The remaining unknown is $Y_{e_{phot}-h}$. In the electron p_T range of interest here, $1.5 < p_T < 4.5 \text{ GeV}/c$ the photonic electrons are dominated by π^0 Dalitz decay and photon conversions [4], where the primary source of the photons which convert is $\pi^0 \rightarrow \gamma\gamma$ decay. We then measure inclusive photon-hadron correlations, where the inclusive photons are dominantly from π^0 decay. Simulations are used to construct $Y_{e_{phot}-h}$ from $Y_{\gamma_{inc}-h}$:

$$Y_{e_{phot}-h}(p_{T,i}) = \sum_j w_i(p_{T,j}) Y_{\gamma_{inc}-h}(p_{T,j}) \quad (3)$$

where each i and j represents a bin in electron or photon p_T , respectively, $0.5 \text{ GeV}/c$ wide.

Two methods are used to determine the $w_i(p_{T,j})$ coefficients. In the first method the measured inclusive photon spectrum in p+p collisions is input into a GEANT based simulation of the PHENIX detector. The same electron identification cuts as in the real data analysis are then applied to reconstructed conversion electrons and the relationship between the input photon p_T and the reconstructed conversion electron p_T determines w . In the second method, the measured π^0 spectrum from [5] is taken as input to a Monte Carlo simulation which decays the π^0 s via their Dalitz decay. The relationship between the intermediate off-shell photon and the

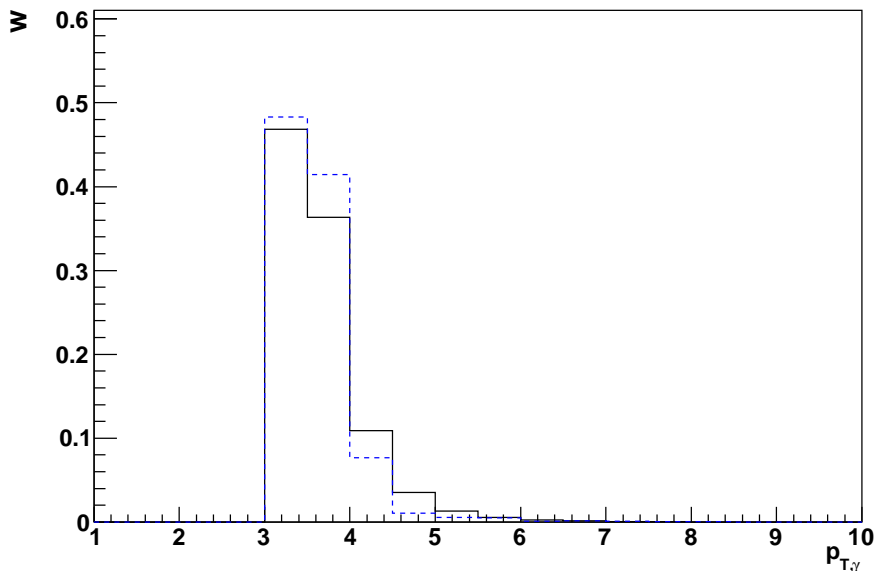


Fig. 1. w for electrons with $3.0 < p_T < 3.5 \text{ GeV}/c$ from the method using Dalitz decays (black solid line) and photon conversions (blue dashed line) as a function of the photon p_T .

resulting electron are used in the same manner as in the first method to determine w . The resulting weights are shown in Fig. 1 for a single electron p_T selection. The difference between the two methods is small. The π^0 spectrum falls steeply with p_T and thus the measured photonic electrons at a given p_T are dominated by those carrying a large fraction of the π^0 p_T regardless of whether the electron comes from a conversion or a Dalitz decay.

The measured conditional yields are corrected for the hadron acceptance and reconstruction efficiency by comparing the raw measured hadron p_T spectrum to the corrected spectrum in Ref. [6]. The non-uniform azimuthal acceptance in PHENIX is corrected for by using mixed pairs. The jet functions are obtained by subtracting the combinatoric background by the zero yield at minimum (ZYAM) [7] method.

The electrons were identified as in Refs. [4, 8]. The systematic errors are from the different methods used to construct $Y_{e_{phot}-h}$, the statistical error on the determination of the ZYAM level which moves all points by the same amount in a given $p_{T,e}$ and $p_{T,h}$ combination. For $Y_{e_{HF}-h}$ there is an additional uncertainty from the R_{HF} value used to subtract the jet functions. These systematic errors are shown the grey boxes in the plots that follow. The systematic error on the efficiency correction is 10% and moves all conditional yield measurements together and is not

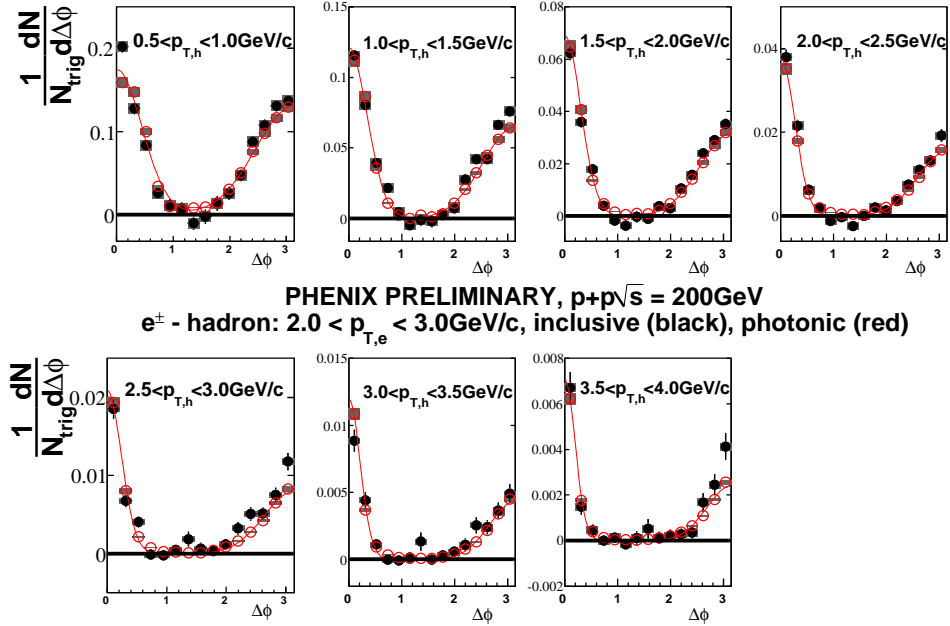


Fig. 2. Efficiency corrected $e_{inc} - h$ jet functions (solid black) and $e_{phot} - h$ jet functions (hollow red) conditional yields for electrons with $2.0 < p_T < 3.0\text{GeV}/c$ and seven hadron p_T bins from 0.5-4.5GeV/c.

shown on the plots.

3. Results

Fig. 2 shows the corrected jet functions for inclusive electrons with $2.0 < p_T < 3.0\text{GeV}/c$ and seven hadron p_T bins. The constructed photonic electron jet functions are shown in the hollow points. The fits shown are to near and away side Gaussians with a flat background. The resulting $e_{HF} - h$ jet functions are extracted using Eq. 2 and are shown in Fig. 3.

In heavy quark fragmentation most of the quark momentum is carried by the heavy meson [9, 11], thus the near side $e_{HF} - h$ is expected to be dominated by pairs in which both particles come from the heavy meson decay. Due to the decay kinematics, we then expect the Gaussian widths of the near side to be wider for $e_{HF} - h$ than $e_{inc} - h$. The widths from both categories of electrons are shown in Fig. 4. The measured near side widths for $e_{HF} - h$ are wider than $e_{phot} - h$ and are in agreement with widths from charm production in PYTHIA [14].

The jet functions are then integrated to get near and away side conditional

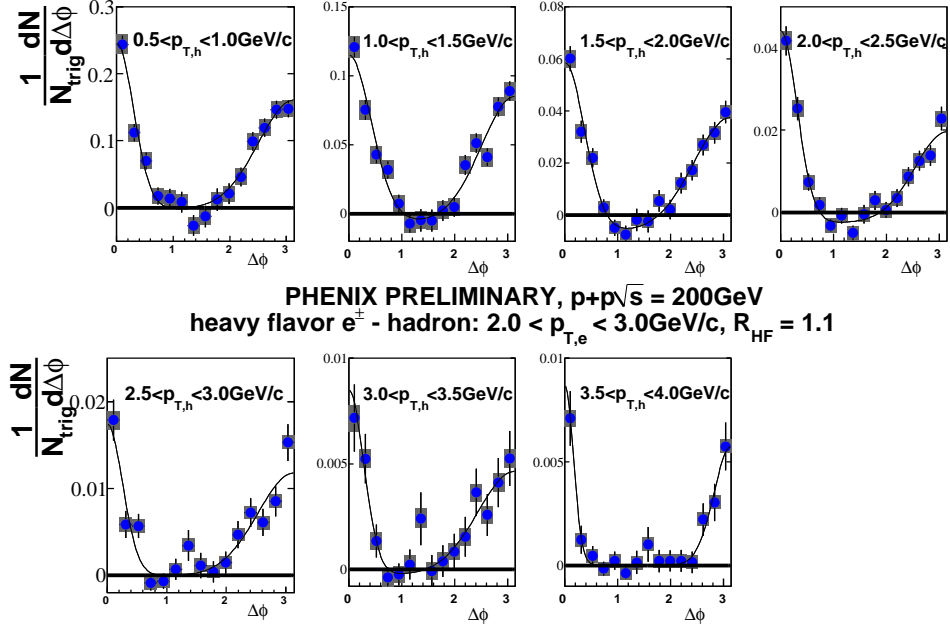


Fig. 3. $Y_{e_{HF}} - h$ conditional yields following the subtraction in Eq. 2 for $2.0 < p_{T,e} < 3.0 \text{ GeV}/c$ and seven hadron p_T bins from 0.5-4.5 GeV/c. In this p_T bin $R_{HF} = 1.1$.

yields of hadrons per trigger heavy flavor electron. The near side integration range is $0 < \Delta\phi < 1.25$ rad and the away side integration range is $1.67 < \Delta\phi < \pi$ rad. The conditional yields are shown in Fig. 5.

The left panel of Fig. 6 shows the away side conditional yields for the data as a function of $p_{T,hadron}/p_{T,e}$ along with exponential fits. For comparisons we also show the same distributions and fits for a PYTHIA simulation of charm production (MSEL=4). The negative slopes are shown from the data and PYTHIA are shown in the right panel of Fig. 6. The ratio $p_{T,hadron}/p_{T,e}$ is defined as z_T for the light flavor jets. We can compare the away side slopes measured here to those measured in Fig. 19 of Ref. [1] for $\pi^0 - h$ correlations. At the same $p_{T,trig}$ the $e_{HF} - h$ slopes are harder than the $\pi^0 - h$. However, in both cases the $p_{T,trig}$ is not the $p_{T,parton}$.

Since the current measurements are at low p_T where sizable contributions of electrons from charm quarks the PYTHIA comparisons made here are only for charm production. In order to make more detailed comparisons, it is necessary to include bottom quarks as well in addition to including next to leading order effects not included in PYTHIA. A further complication is that the heavy flavor quark that leads to a trigger is not necessarily balanced by an away side balancing heavy quark. Ref [15] shows a leading order calculation of the subprocess leading to mid-rapidity

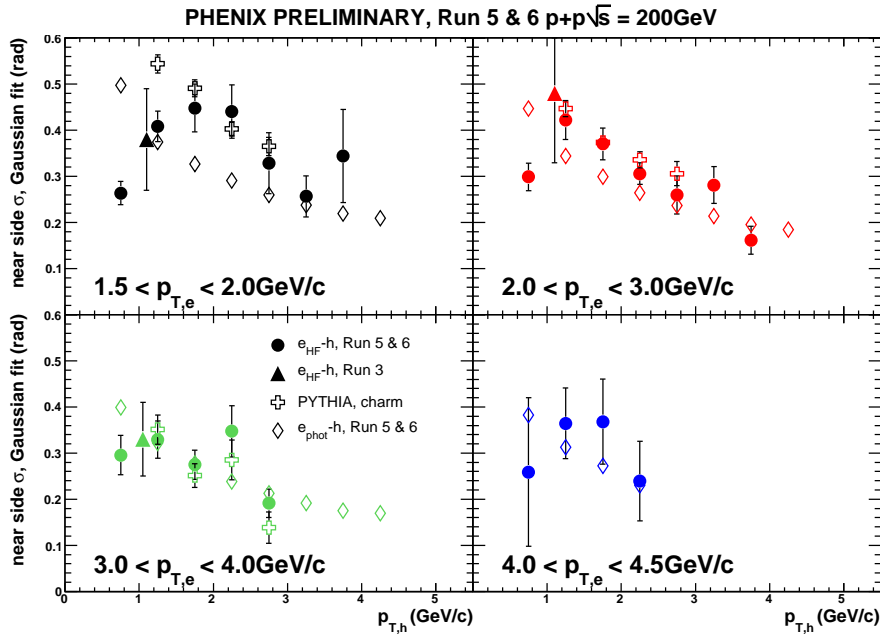


Fig. 4. Gaussian widths as a function of p_T, h for four electron p_T bins. Circles show the $e_{HF} - h$ widths and open diamonds show $e_{phot} - h$ widths. Pluses show $e_{HF} - h$ widths from PYTHIA and the triangles show an earlier PHENIX measurement of $e_{HF} - h$ widths with lower statistics and $1.0 < p_T < 4.0 \text{ GeV}/c$.

D production and finds that in the p_T range relevant here $gg \rightarrow c\bar{c}$ contributes $\approx 20\%$ and the rest of the contribution is from processes such as $cg \rightarrow cg$ or $cq(\bar{q}) \rightarrow cq(\bar{q})$. These processes are included in next to leading order calculations where there are three partons in the final state [16]. However the PYTHIA simulations here only include $gg \rightarrow c\bar{c}$. Further studies using NLO Monte Carlo calculations are necessary to understand the partonic contribution to the away side jets.

4. Conclusions and Outlook

Jet physics with heavy flavor is an important new frontier in heavy ion physics. Heavy flavor triggered two particle correlations provide complementary information to π^0 and direct photon triggered measurements. However the measurements are difficult because of the background from photon conversions and light meson Dalitz decays. We have shown a new method which allows the extraction of correlations triggered by electrons from heavy flavor decay and showed preliminary results from proton-proton collisions. These measurements are an essential baseline for

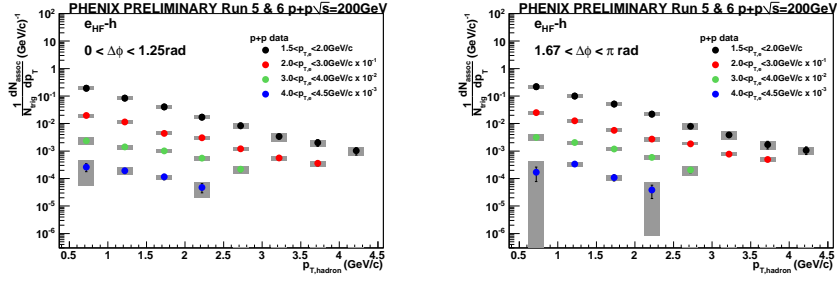


Fig. 5. Near (left) and away (right) side conditional yields for $e_{HF} - h$ correlations for four electron p_T bins and eight hadron p_T bins.

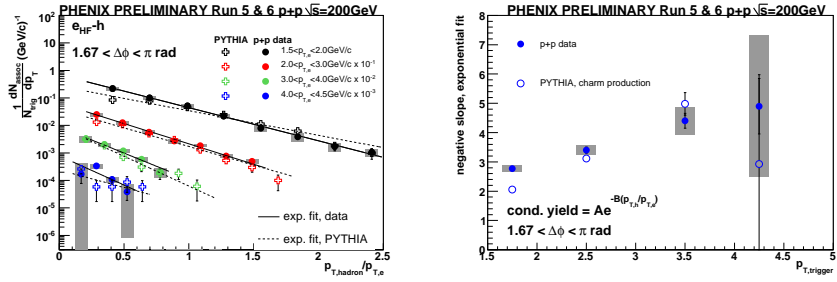


Fig. 6. (left) Away side conditional yield measurements as a function of $p_{T,hadron}/p_{T,e}$. Fits for the data and the PYTHIA are to exponentials. (right) Negative slopes from the data and PYTHIA fits.

understanding heavy ion results. These measurements are crucial to understanding the interactions between heavy quarks and the hot nuclear matter produced in relativistic heavy ion collisions.

Current measurements are limited by statistics and by the inability to separate the correlations from charm and bottom quarks. Silicon vertex detector upgrades and higher luminosity data will greatly help these measurements. Additionally, these types of measurements will be very interesting at the Large Hadron Collider.

Preliminary results presented at the conference on extracting the relative contributions to the electron spectrum from c and b quarks have been superseded by final results, submitted for publication [8].

References

1. S. S. Adler et al., *Phys. Rev.* **D74** (2006) 072002
2. A. Adare et al., *Phys. Rev. Lett.* **98** (2007) 172301
3. A. Adare et al., *submitted to Phys. Rev C*
4. A. Adare et al., *Phys. Rev. Lett* **97** (2006) 252002
5. S. S. Adler et al., *Phys. Rev. Lett.* **91** (2003) 241803
6. S. S. Adler et al., *Phys. Rev. Lett.* **95** (2005) 202001
7. A. Adare et al., *Phys. Rev* **C78** (2008) 014901
8. A. Adare et al., *submitted to Phys. Rev. Lett.*
9. M. Artuso et al., *Phys. Rev* **D70** (2004) 112001
10. R. Seuster et al., *Phys. Rev.* **D73** (2006) 032002
11. A. Heister et al., *Phys. Lett.* **B512** (2001) 30
12. G. Abbiendi et al., *Eur. Phys. J.* **C29** (2003) 463
13. K. Abe et al., *Phys. Rev* **D65** (2002) 092006
14. T. Sjostrand et al., *Comp. Phys. Comm* **135** (2001) 238
15. I. Vitev et al., *Phys Rev* **D74** (2006) 054010
16. P. Nason, S. Dawson and R. K. Ellis, *Nucl. Phys.* **B303** (1988) 607.